DNA–Nogalamycin Interactions[†,‡]

Martin Egli, Loren Dean Williams, Christine A. Frederick, and Alexander Rich*

Department of Biology, Massachusetts Institute of Technology, Cambridge, Massachusetts 02139

Received August 15, 1990; Revised Manuscript Received October 17, 1990

ABSTRACT: The anthracycline antibiotic nogalamycin differs from the more common daunomycin-type anthracyclines by substitution on both ends of the intercalating chromophore, giving nogalamycin the approximate shape of a dumbbell. The chromophore of daunomycin is substituted on only one end. In nogalamycin, the positively charged amino sugar substituent of daunomycin is replaced by an uncharged nogalose sugar and a methyl ester group. The other end of nogalamycin, where daunomycin is unsubstituted, is fused to a bicyclo amino sugar with a positively charged dimethylamino group. Much larger DNA fluctuations are required for intercalative entry of nogalamycin than for entry of daunomycin. This report describes the X-ray crystal structure of the complex between nogalamycin and the self-complementary DNA hexamer d(^{me5}CGTsA^{me5}CG). The DNA contains cytosines methylated at the 5-positions and a phosphorothioate linkage at the TpA step. Nogalamycin intercalates at the terminal CpG steps and interacts with both strands in both grooves of the DNA. Large conformational adjustments in both nogalamycin and the DNA are necessary to form a stable, intercalative complex. The interactions of the bases with the nogalamycin substituents lead to sliding of bases relative to each other along the normal to Watson–Crick hydrogen bonds. The planarities of base pairs surrounding the intercalation site are distorted. The backbones of the two strands are distorted asymmetrically by nogalamycin with large deviations from standard B-DNA geometry. The complex between nogalamycin and DNA illustrates the conformational flexibility of DNA. The hydrogen-bonding interactions between nogalamycin and DNA do not suggest a sequence-specific binding of the drug, although additional secondary effects might lead to differences between various intercalation sites.

$\mathbf{A}$nthracyclines constitute a widely used family of chemotherapeutic agents. The clinical properties of these DNA binding agents strongly depend on minor chemical modifications (Brown, 1983; Acramone & Penco, 1988). The anthracycline daunomycin is effective for treating acute leukemia while adriamycin, which differs by an additional hydroxyl group, is more effective for treating solid tumors. The recently developed 4'-epiadriamycin, which differs from adriamycin by inversion of the stereochemistry at another hydroxyl group, is better tolerated and is now in clinical use in Europe (Acramone & Penco, 1988). The daunomycin class of anthracyclines is composed of a planar chromophore substituted on only one end. The substituent is a positively charged amino sugar.

Nogalamycin (Figure 1A), isolated from *Streptomyces nogalator* var. *nogalator*, is larger and more complex than daunomycin. Nogalamycin selectively inhibits DNA-directed RNA synthesis in vivo (Fok & Waring, 1972; Li et al., 1979; Ennis, 1981) and is active against Gram-positive bacteria and experimental tumors (Bhuyan, 1967; Bhuyan & Reusser, 1970; Li et al., 1979). This drug is composed of a planar chromophore substituted on both ends and assumes the approximate shape of a dumbbell (Figure 1B). On one end of the chromophore, nogalamycin contains both a methyl ester and a nogalose sugar, which is uncharged. The other end of the chromophore is fused to a bicyclo amino sugar containing a

positively charged dimethylamino group.

In spite of the mechanistic obstacle presented by the dumbbell shape of nogalamycin, the drug forms a stable, intercalative complex with DNA (Kersten et al., 1966; Waring, 1970; Das et al., 1974; Sinha et al., 1977; Plumbridge & Brown, 1979; Gale et al., 1981; Searle et al., 1988; Williams et al., 1990a; Zhang & Patel, 1990). The slow association and dissociation rates (Fok & Waring, 1972; Fox et al., 1985) are consistent with the suggestion that transient DNA melting is required for entry of nogalamycin into the duplex (Collier et al., 1984). In an alternative mechanism of binding, we have suggested the possibility that an opening to allow entry of nogalamycin could be created by unstacking and buckling of DNA base pairs without hydrogen bond disruption (Williams et al., 1990a). In this mechanism, the DNA fluctuations would be of greater amplitude than required for entry of simpler intercalators such as daunomycin. However, it is necessary to alter the conformation of nogalamycin to facilitate entry into the unstacked DNA. The conformation of the A ring (Figure 1A) must adjust such that the bulky substituents flip to equatorial positions rather than the axial positions in Figure 1B.

We have previously described in a preliminary fashion the molecular structure of the complex formed by nogalamycin bound to the self-complementary DNA hexamer d(^{me}CGTsA^{me}CG) (Williams et al., 1990a). A related complex without the methyl groups and in a slightly different crystal form has also been described in a preliminary fashion (Liaw et al., 1989). As shown in Figure 2, one molecule of nogalamycin intercalates at each of the two ^{me}CpG steps of the hexamer duplex. Nogalamycin threads between the phosphodiester backbones and interacts with both strands in both grooves of the DNA. The long axis of the chromophore is roughly perpendicular to that of the base pairs, and the three aromatic rings (B–D) are stacked within the DNA while cyclohexene

---

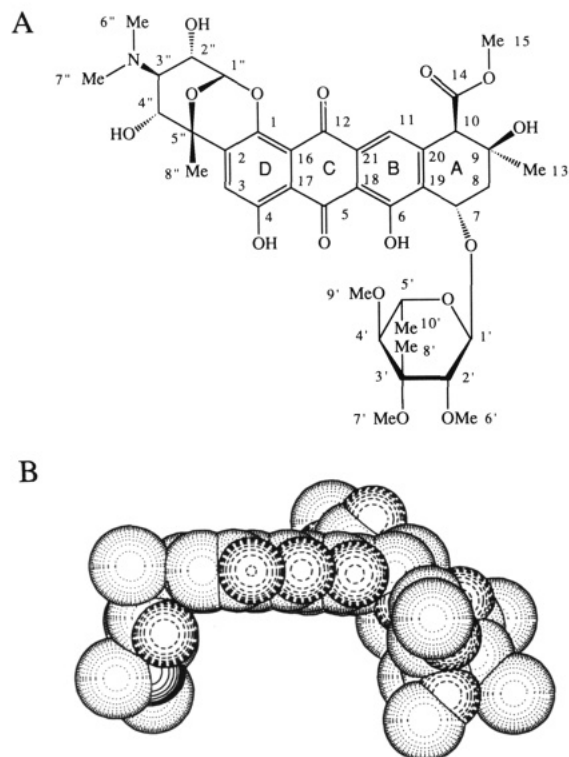*To whom correspondence should be addressed.

FIGURE 1: (A) Numbering scheme for nogalamycin. (B) Space-filling representation of nogalamycin. The chromophore is perpendicular to the plane of the paper, the bicyclo amino sugar is on the left, and the nogalose sugar is on the right. Carbon atoms are dotted, oxygen atoms are dashed, and nitrogen atoms are concentric circles.
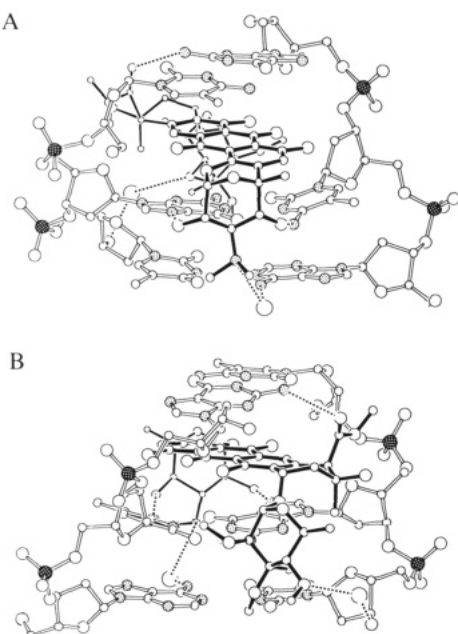

FIGURE 2: ORTEP drawings of the complex viewed from (A) the major groove and (B) the minor groove. The DNA is drawn with open bonds and nogalamycin with solid bonds. Phosphorus atoms are stippled in black, nitrogen atoms are stippled in grey, and water molecules are the largest circles. Water-mediated hydrogen bonds and hydrogen bonds between nogalamycin and DNA are dashed lines.

ring A is completely unstacked and protrudes into the minor groove. In this report, we describe our complex in full detail with a complete analysis of the structure.

MATERIALS AND METHODS

Crystals were grown at room temperature in sitting drops according to the vapor diffusion method. The crystallization
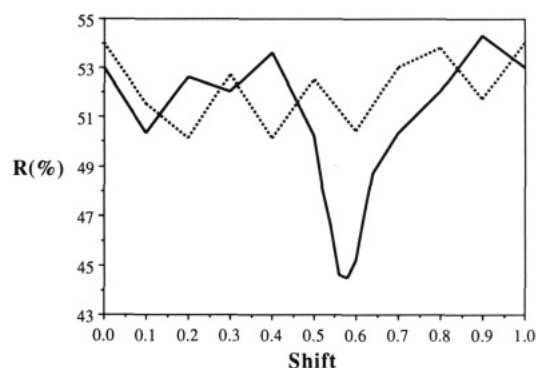

FIGURE 3: *R* factors of structure factor calculations when shifting the daunomycin–d(CGTACG) complex coordinates along the dyad through $(^1/_2, 0, ^1/_4)$ in space group $P6_122$, using 3-Å nogalamycin data. A shift of 0 corresponds to the position of the duplex at $(^1/_2, 0, ^1/_4)$, and dashed and solid lines represent two orientations of the complex which differ by a 180° rotation around the crystallographic *c* axis.

parameters, including DNA length, sequence, and sulfur modification, which yielded diffraction quality crystals were established as described previously (Williams et al., 1990a). The DNA–nogalamycin complex crystallized in space group $P6_122$ with unit cell dimensions $a = b = 26.30$ Å and $c = 100.01$ Å. Data collection and reduction were described previously.

Patterson maps revealed the orientation of the duplexes in the cell with the helical axis parallel to the *xy* plane. Symmetry considerations suggested that the duplex adopted crystallographic 2-fold symmetry with one strand of the DNA and one drug molecule in the asymmetric unit. It was therefore possible to derive the rough position of the complex by shifting a model along the 2-fold rotation axis and performing a series of structure factor calculations. The daunomycin–d(CGTACG) complex (Quigley et al., 1980) was used as a model and was translated along the 2-fold axis in steps of 2.0 Å, calculating structure factors at every step, using data between 10- and 3-Å resolution. Two orientations of the duplex corresponding to a rotation by 180° about the *c* axis were evaluated in this manner. The rotationally and translationally correct position was suggested by a distinct minimum at a shift of 0.58 (fractional) for one of the duplex orientations but not the other (Figure 3). By use of the model in this orientation and position, Fourier sum $(2F_{obs} - F_{calc})$ and difference maps $(F_{obs} - F_{calc})$ displayed on an Evans & Sutherland PS390 graphics terminal with program FRODO (Jones, 1978) then showed nearly continuous electron density around the DNA backbone and bases.

The next stage consisted of extensive model building as the absolute configuration of nogalamycin was unknown and all of the possible orientations with respect to the DNA had to be evaluated. Arora had determined the relative configuration of nogalamycin by X-ray analysis (Arora, 1983). The configuration of the A ring was either 7*S*,9*S*,10*R* or 7*R*,9*R*,10*S*. Both enantiomers were evaluated in four different orientations at the CpG step of the duplex. The 7*S*,9*S*,10*R* enantiomer, bound to the DNA with the chromophore intercalated at the CpG step and the nogalose and bicyclo amino sugars oriented toward the center of the duplex, resulted in the lowest *R* factors and considerably better electron density sum and difference maps compared to other models.

In the initial refinement, the Konnert–Hendrickson least-squares procedure (Hendrickson & Konnert, 1981), as modified for nucleic acids (Quigley et al., 1978), was used with tight stereochemical constraints. At an *R* factor of 24% (in-
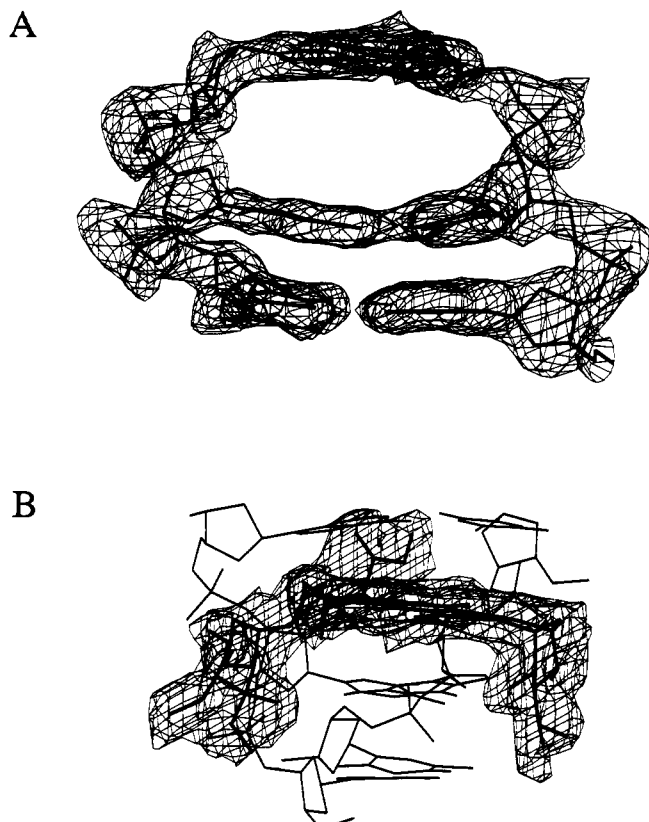
A

B

FIGURE 4: Electron density sum map of (A) the DNA alone and (B) the nogalamycin molecule alone. The bonds of molecules around which electron density is shown are drawn with thick lines; bonds of the remaining parts of the complex are drawn with thin lines.

Table I: Selected Torsion Angles for Nogalamycin

torsion angle (deg)	free drug (Arora, 1983)	DNA complex (this work)	Δ
amino sugar			
C16–C1–O1–C1″	−173	170	17
O1–C1″–C2″–O2″	−56	−59	3
C4–C3–C2–C5″	−172	166	22
C2–C5″–C4″–O4″	64	50	14
C16–C1–C2–C5″	169	−168	23
C3–C2–C1–O1	176	173	3
methyl ester			
C20–C10–C14–O10	−127	−107	20
glycosyl linkage			
C8–C7–O7–C1′	105	111	6
C19–C7–O7–C1′	−137	−130	7
C7–O7–C1′–O1′	−73	−83	10
C7–O7–C1′–C2′	164	151	13
A ring			
C21–C11–C20–C10	−178	−177	1
C11–C20–C10–C9	−165	−165	0
C20–C10–C9–C8	−48	−45	3
C10–C9–C8–C7	61	62	1
C9–C8–C7–C19	−39	−44	5
C8–C7–C19–C6	−169	−165	4
C7–C19–C6–C18	174	176	2
C7–C19–C20–C11	−173	−176	3
C6–C19–C20–C10	179	177	2

asymmetric unit, and the calculated density is 1.08 g/cm³ with an ordered water content of 22% w/w. The electron density maps showed clean and continuous density around the complex (Figure 4); however, it was impossible to assign the absolute configuration of the chiral phosphorus atoms at the TpA steps. The sulfur atom was therefore treated as an oxygen atom.

RESULTS

Conformation and Interactions of Nogalamycin. The conformation of nogalamycin when bound to DNA is substantially different from the conformation of free nogalamycin. For the conformation of free nogalamycin, we have used the X-ray crystal structure of nogalamycin alone (Arora, 1983). Nogalamycin in the free state is superimposed on the bound state in Figure 5, and selected torsion angles of the two states are listed in Table I. Upon binding to DNA, the bicyclo amino sugar shifts down (in Figure 5), away from the plane of the chromophore, and bends in toward the center of the nogalamycin molecule. This conformational adjustment shifts the bicyclo amino sugar toward the floor of the major groove and places the O2″ and O4″ atoms in favorable positions for hydrogen bonding to the G(2)·C(11) base pair. The O2″ donates in a hydrogen bond to the N7 of G(2), and the O4″ receives in a hydrogen bond to the N4 of C(11) (Figure 2, Table II). Compared to the free molecule, the total positional shift of O2″ is 0.6 Å while that of O4″ is 1.6 Å. This realignment of the position of the bicyclo amino sugar is accom-

cluding most of the water molecules), the nogalose sugar was still poorly resolved and some of the bond lengths and bond angles in the drug were unreasonable. The nogalose was then rebuilt, and the program XPLOR (Brünger et al., 1987) was used for further refinement. The system was first equilibrated at 2000 K for 1 ps (ps) in steps of 1 fs (fs). The annealing process was performed in 34 stages with 50 steps of molecular dynamics (0.5 fs) at each stage. The target temperature of the system was decreased in increments of 50 K between stages to a final temperature of 300 K. The system was then energy minimized for 300 steps by using the CHARMM (Brooks et al., 1983) potential with restraints from the crystallographic data. Finally, individual temperature factors were refined (unrestrained) for 200 additional steps.

Sum and difference maps then showed the complete nogalamycin molecule to be in electron density. After subtle corrections of several water molecule positions and additional refinement, the R factor converged at 20.6% at 2.0-Å resolution. The final structure contained 39 water molecules per
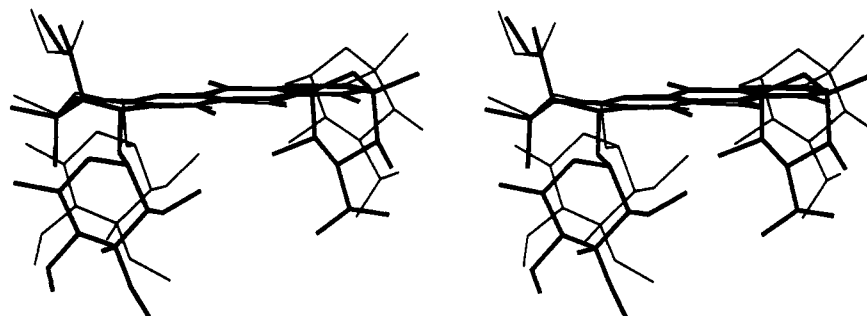

FIGURE 5: Stereo drawing of the crystal structure of nogalamycin alone (thin lines) superimposed on nogalamycin from the DNA complex (thick lines). The chromophore was used for the superposition.

Table II: Hydrogen Bonds (*) and Short Contacts (<3.3 Å) between Nogalamycin and DNA

nogalamycin	DNA	distance (Å)
C6	G(12) N3	3.17
C11	G(2) N3	3.28
C12	G(2) C5	3.17
C15	C(1) C2′	3.23
O1	G(2) N7	3.26
O4	C(11) C6	3.24
	C4	3.07
	C5	2.85
O5	C(11) C2	3.28
O6	G(12) C4	3.12
O10	G(2) O1′	3.25
O14	G(12) N2	2.94*
C7′	A(4) O1′	3.11
O2″	G(2) N7	2.63*
C3″	G(2) O6	3.07
O4″	C(11) N4	2.58*

Table III: Rotational and Translational Parameters for Base Pairs and Base Pair Steps[a,b]

tip (deg)	incl (deg)	twist (deg)	roll (deg)	tilt (deg)
−9.8	−2.6	35.6	6.0	1.9
−1.2	−4.5	24.8	−4.0	−1.5
−2.7	−7.2	39.4	0.3	0.0
2.7	−7.2	24.8	−4.0	1.5
1.2	−4.5	35.6	6.0	−1.9
9.8	−2.6			

propeller twist (deg)	buckle (deg)	slide (Å)	x displacement (Å)	y displacement (Å)
−4.4	−10.9	0.3	0.9	0.3
−1.6	26.2	−0.1	1.1	0.2
−4.3	8.5	−1.1	−0.1	0.2
−4.3	−8.5	−0.1	−0.1	−0.2
−1.6	−26.2	0.3	1.1	−0.2
−4.4	10.9		0.9	−0.3

[a] Columns with only five values refer to parameters between base pairs. [b] Were obtained with the program NEWHELIX (Dickerson et al., 1989).
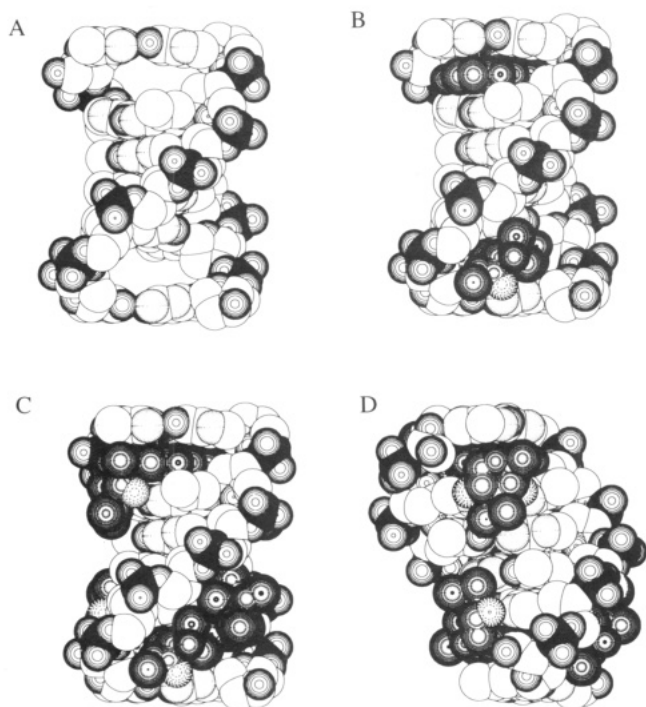

FIGURE 6: Space-filling representations of the complex of nogalamycin plus d(^{me}CGTsA^{me}CG). (A) Viewing across major and minor grooves with nogalamycin completely omitted. (B) Same view including the chromophore of nogalamycin. (C) Same view of the complex including the complete nogalamycin molecule. (D) View into the major groove of the complex including the complete nogalamycin molecule. In the DNA, carbon atoms are white, nitrogen atoms are dotted, oxygen atoms are circled, and phosphorus atoms are black. In nogalamycin, concentric circles with radial lines were used for all atoms except for the two hydroxyl oxygens in the bicyclo amino sugar and the carbonyl oxygen of the methyl ester group, which are dashed.

plished by torsional rotations primarily about three bonds of nogalamycin, C16–C1–O1–C1″ (17°), C4–C3–C2–C5″ (22°), and C16–C1–C2–C5″ (23°). At the other end of the nogalamycin molecule, a torsional rotation about the C20–C10–C14–O10 bond (20°) similarly serves to shift the carbonyl oxygen (O14) to a position closer to the center of the nogalamycin molecule. This realignment shifts the position of O14 by 0.8 Å toward the floor of the minor groove to a position more favorable for hydrogen bonding to the N2 of G(2).

The DNA forms a wedge-shaped cavity for the nogalamycin chromophore as can be seen in the space-filling representation of the DNA with the drug omitted (Figure 6A). The shape of the cavity allows for extensive van der Waals contact between the DNA and the chromophore (Table II). The van der Waals contacts can be seen in the space-filling representation of the DNA plus the chromophore in Figure 6B, where the nogalose and bicyclo amino sugar have been omitted. Nogalamycin interacts in both grooves and with both strands of the duplex. Space-filling representations of the complete DNA–nogalamycin complex are shown in Figure 6, panels C (view across the major and minor grooves) and D (view into the major groove). Although the nogalose nearly fills the minor groove, there is only a single van der Waals contact with the DNA, between C7′ and O1′ of A(4) (Table II). However, nogalamycin also interacts in the minor groove via the O14 of the methyl ester which forms a hydrogen bond to the N2 of the terminal G(12). The DNA partially compensates for the poor fit of nogalamycin by shifting residue G(12) into the minor groove, away from optimal base pairing geometry with C(1). This shift is stabilized by the hydrogen bond with the methyl ester of nogalamycin. In the major groove, the bicyclo amino sugar forms strong hydrogen bonds to both bases of the G(2)·C(11) base pair (as described above). The hydrogen bond to O4″ shifts C(11) into the major groove, away from optimal base pairing geometry with G(2), resulting in close contacts with a hydroxyl oxygen (O4) of the nogalamycin chromophore (Table II).

Base Stacking Interactions. Characteristic changes in stacking interactions are associated with intercalation of nogalamycin. Figure 7 shows the stacking of each dinucleotide step starting at one end of the duplex and moving to the center. The first step is formed by the terminal C·G base pair of one duplex stacking on the terminal C·G base pair of an adjacent duplex in the crystal (Figure 7A). The two duplexes, which are related by a crystallographic 2-fold rotation, stack with nearly complete 3′,3′ and 5′,5′ overlap. In contrast, in tetragonal lattices formed by complexes of daunomycin-type anthracyclines with various DNA hexamers (Wang et al., 1987; Frederick et al., 1990) the overlaps are of the 3′,5′ and 5′,3′ type, similar to the normal stacking observed within B-DNA helices. However, in the X-ray crystal structure of 11-deoxydaunomycin bound to DNA containing a phosphorothioate linkage (Williams et al., 1990b), the duplexes stack in the same 3′,3′ and 5′,5′ manner as in the nogalamycin complex.

The terminal base pair, adjacent to the chromophore is distorted along the helical axis by a buckle of nearly −11° while the base pair on the other side of the chromophore buckles in the other direction, by 26° (Table III). However, the
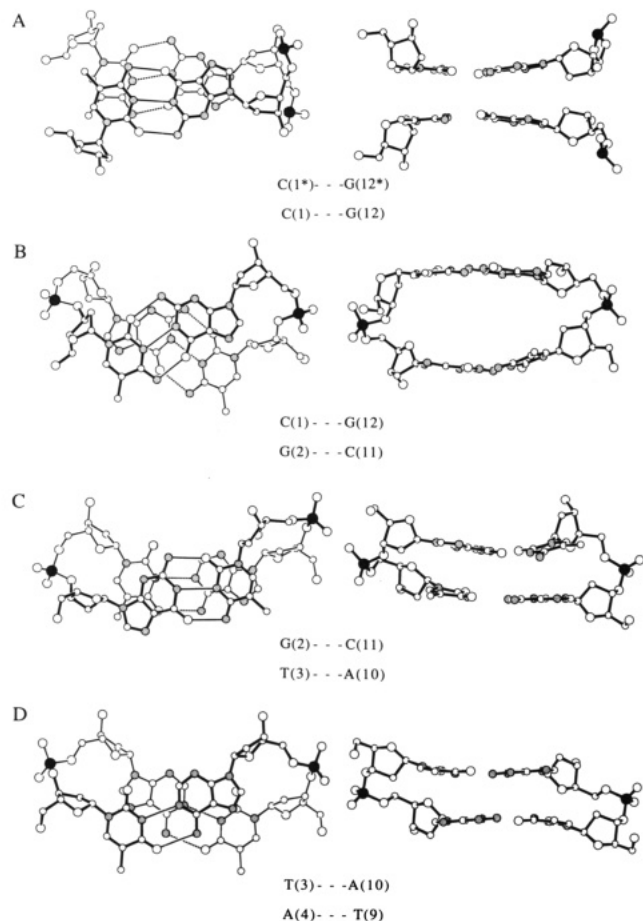
FIGURE 7: Base-paired dinucleotide steps. Left: View along the helical axis (normal to the best plane through the upper base pair). Right: View into the major groove (previous view rotated 90° around the horizontal). (A) Terminal C·G base pair of one duplex stacked on the terminal C·G base pair of the next duplex, showing the 3,3′ step. The two base pairs are related by a crystallographic 2-fold rotation. (B) CpG intercalation step with the nogalamycin molecule omitted, displaying the severe buckle in both base pairs. (C) GpT step adjacent to the intercalation site. (D) Central TpA step with almost standard B-DNA geometry. The two base pairs are related by a crystallographic 2-fold rotation. The top base pair is drawn with thick lines, and the bottom base pair is drawn with thin lines. Nitrogen atoms are stippled in grey, and phosphorus atoms are stippled in black. In the left column, hydrogen bonds in the top base pairs are solid lines and hydrogen bonds in the bottom base pair are dashed lines.

propeller twists in the nogalamycin complex are small (<5°, Table III). The sliding of bases relative to each other, along the normal to the Watson–Crick hydrogen bonds (shear), is large in the nogalamycin complex (Figure 7B,C, left).

Backbone Conformation. When viewing along the axis of the helix, unwinding of DNA appears to cause the ribose of one residue to shift toward the ribose of the next residue of the same strand. Unwinding is symmetric and leads to similar ribose shifts on both strands of the duplex when the strand is viewed along the helix axis. However, in the nogalamycin–DNA complex, displacement of base pairs in their planes has resulted in asymmetric shifts of the riboses.

In the C(1)·G(12)–G(2)·C(11) step of the nogalamycin complex, one strand shifts by displacement of the C(1)·G(12) base pair (Figure 7B, left). The guanine of G(12) is displaced toward the minor groove by the hydrogen bond between N2 of G(12) and O14 of the ester group of nogalamycin. The C(1)–G(2) strand shifts significantly to maintain reasonable geometry in the base pair while the other strand is less shifted. This asymmetry partially accommodates the shift of G(12) but does not completely prevent the base pair from shearing.

Table IV: Phosphorus–Phosphorus Distances in Å

adjacent atoms		
G(2) P–T(3) P = G(8) P–T(9) P		6.4
T(3) P–A(4) P = T(9) P–A(10) P		6.8
A(4) P–C(5) P = A(10 P–C(11)P		6.7
C(5) P–G(6) P = C(11) P–G(12) P		6.6
	$\sum/n = 6.6$	
G(2) P–G(8) P		15.9
(corresponding to major groove width)[a,b]		
A(4) P–G(12) P		8.8
C(5) P–C(11) P		7.6
G(6) P–A(10) P		8.8
	$\sum/n = 8.4$	
(corresponding to minor groove width)[a,b]		

[a] As defined by Conner et al. (1982). [b] Distances minus 5.8 Å, the sum of the phosphate van der Waals radii.

In the G(2)·C(11)–T(3)·A(10) step, the other strand [the A(10)-C(11) strand] is shifted (Figure 7C, left). The asymmetric shift at this step is related to a hydrogen bond between N4 of C(11) and O4″ of the bicyclo amino sugar which displaces the cytosine of C(11) toward the major groove. As described for the previous step, the asymmetric shift partially accommodates the displacement but does not completely prevent the G(2)·C(11) base pair from shearing.

The asymmetry of the two backbones is illustrated by differences in their torsion angles [reported previously in Williams et al. (1990a)].[1] Starting with the torsion angle δ at the base pair step C(1)·G(12)–G(2)·C(11) and calculating the absolute differences between torsion angles of opposite strands when going from 5′ to 3′ (for both strands), we obtain the following angles in degrees: $\Delta\delta[1,11] = 24$, $\Delta\epsilon[1,11] = 99$, $\Delta\zeta[1,11] = 7$, $\Delta\alpha[2,12] = 105$, $\Delta\beta[2,12] = 216$, $\Delta\gamma[2,12] = 217$, and $\Delta\delta[2,12] = 18$. In general, C(1)–G(2) is closer to standard B-DNA [as defined in Saenger (1984)] than C(11)–G(12). Looking at the differences between the same angles within the step G(2)·C(11)–T(3)·A(10) starting with δ, we obtain the following values in degrees: $\Delta\delta[2,10] = 23$, $\Delta\epsilon[2,10] = 293$, $\Delta\zeta[2,10] = 230$, $\Delta\alpha[3,11] = 210$, $\Delta\beta[3,11] = 54$, $\Delta\gamma[3,11] = 115$, and $\Delta\delta[3,11] = 14$. The asymmetry in this step which is visible in Figure 7C is manifested by large differences in torsion angles. The comparison of the torsions of both strand segments with standard B-DNA values suggests that they differ from standard values by similar extents. Consistent with the crystallographic 2-fold symmetry, the T(3)·A(10)–A-(4)·T(9) step is very regular and the torsion angles in both strands are the same. The geometry of this step is very close to that of B-DNA. The absolute differences to the standard values in degrees are as follows: $\Delta\delta[3] = 20$, $\Delta\epsilon[3] = 11$, $\Delta\zeta[3] = 35$, $\Delta\alpha[4] = 16$, $\Delta\beta[4] = 10$, and $\Delta\gamma[4] = 7$.

Despite distortions of the backbones, the phosphorus–phosphorus distances are surprisingly regular. The distances between adjacent phosphorus atoms are listed in Table IV. The distances between phosphorus atoms P5 and P6 and P11 and P12 at the intercalation steps are similar to those between phosphorus atoms at the other steps, and all of them are in the range of the distances observed in B-DNA.

Thermal Motion. The isotropic temperature factors (*B* factors) reflect the mobility of atoms within the crystal. Figure 8 shows a major (A) and a minor groove view (B) of the nogalamycin complex plus the first water shell with the shading of the atoms coding for temperature factors. Lighter regions are more rigid, and darker regions are more mobile. As ex-

---

[1] Backbone torsion angles are defined as P–α–O5′–β–C5′–γ–C4′–δ–C3′–ϵ–O3′–ζ–P.
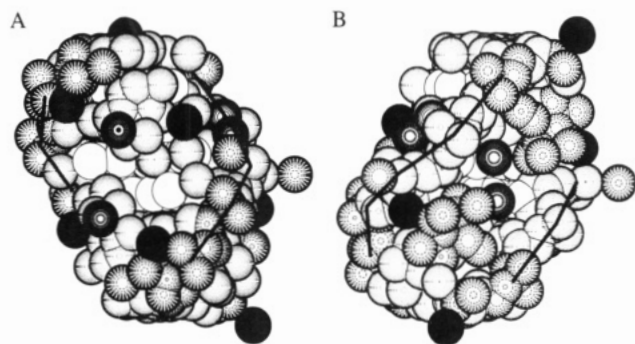
FIGURE 8: (A) Major groove and (B) minor groove of the DNA–nogalamycin complex plus the first water shell, shaded according to temperature factors. Lighter regions correspond to lower temperature factors, and darker regions correspond to higher temperature factors. White, $0 < B < 8$ Å^2; dotted $8 \leq B < 16$ Å^2; dashed, $16 \leq B < 24$ Å^2; circled, $24 \leq B < 32$ Å^2; circled with radical lines, $32 \leq B < 40$ Å^2 and black, $B \geq 40$ Å^2. Solid lines denote the DNA backbone. Panel A may be compared to Figure 6D to differentiate between DNA–nogalamycin atoms and first shell water molecules.

Table V: First Shell Water Contacts and Water Temperature Factors

water	B (Å^2)	complex	distance (Å)
W 02	23.5	A(10) O2P	3.12
W 04	9.9	G(12) N7	3.15
W 05	35.2	A(10) N3	2.68
W 06	11.0	A(10) N7	3.05
W 08	19.2	A(10) O1P	2.56
W 12	24.2	C(11) O1P	3.28
W 17	23.2	C(1) O5′	2.84
W 20	21.9	G(12) O3′	3.05
W 22	6.8	C(1) O5′	2.61
		G(2) O2P	2.64
W 24	34.7	A(10) O5′	3.19
W 27	42.5	G(12) O3′	3.13
W 28	11.1	G(12) O3′	2.69
		Nog O1′	2.81
W 31	51.5	Nog O4″	2.91
W 33	12.1	T(3) O1P	2.76
W 34	20.6	Nog O3′	3.02
W 35	41.1	T(3) O3′	2.81
		Nog O4′	2.84
W 37	13.2	A(10) N6	2.92
		Nog N1	2.91
W 39	37.9	Nog O2″	3.30

pected, the central parts of the complex, the DNA bases and the chromophore of nogalamycin, are white or dotted regions and are relatively immobile. The two central base pairs have averaged B's of 5.9 Å^2 [T(3)] and 5.1 Å^2 [A(4)]. At the next base pairs from the center the averaged B's for the base atoms are larger, 10.6 Å^2 [G(2)], 9.7 Å^2 [C(5)], 14.1 Å^2 [C(1)], and 10.5 Å^2 [G(6)]. The same pattern is observed with the ribose temperature factors. They are much smaller for the two central riboses (11.0 Å^2 [T(3)], 9.5 Å^2 [A(4)]) than for those closer to the duplex ends: 16.7 Å^2 [G(2)], 14.4 Å^2 [C(5)], 18.2 Å^2 [C(1)], and 15.9 Å^2 [G(6)]. The ribose temperature factors are thus generally higher than those of the bases but are lower than those of the phosphates. The increase in temperature factor with distance from the center of the duplex described for the bases and the riboses is also observed for the phosphate groups. The averaged B's (P, O1P, and O2P) are 8.9 Å^2 for the central phosphate P4, 17.9 Å^2 for P3, 14.3 Å^2 for P5, 21.0 Å^2 for P2, and 18.2 Å^2 for P6. Thus, the increase in thermal motion when going from the center of the complex to the ends is consistent for all the groups. This pattern is seen in Figure 8, where the backbone atoms around the intercalation sites are mostly dashed (more motion), whereas the atoms in the central backbone region are mostly dotted (less motion). All the temperature factors of the chromophore atoms of nogalamycin are low, the average being 5.8 Å^2. In part due to the hydrogen-bonding interactions of atoms O2″ and O4″, the bicyclo amino sugar atoms are relatively immobile and appear dotted in Figure 8A, with an average B of 9.8 Å^2. The minor groove view in Figure 8B shows that the nogalose sugar atoms are mostly dashed, with an average B of 18.1 Å^2, almost twice as large as that of the bicyclo amino sugar. However, the methyl ester group appears lighter than the nogalose in Figure 8B. Here the restricted motion is partly due to hydrogen bond formation of O14 to N2 of G(12) which results in a lower averaged B of 10.5 Å^2 for the ester group atoms.

Solvent Structure. Each phosphate group of the DNA forms hydrogen bonds to at least one water molecule, although in the case of the phosphate of G(12), the distances to water molecules are somewhat long [W11 to O1P of G(12) is 3.56 Å; W36 to O2P of G(12) is 3.71 Å]. The first shell water molecules, their distances to the complex, and thermal factors are listed in Table V.

There are four examples of multidentate hydrogen bonding to water molecules in the nogalamycin–DNA complex. Water molecule 22 donates protons in hydrogen bonds to the O5′ of
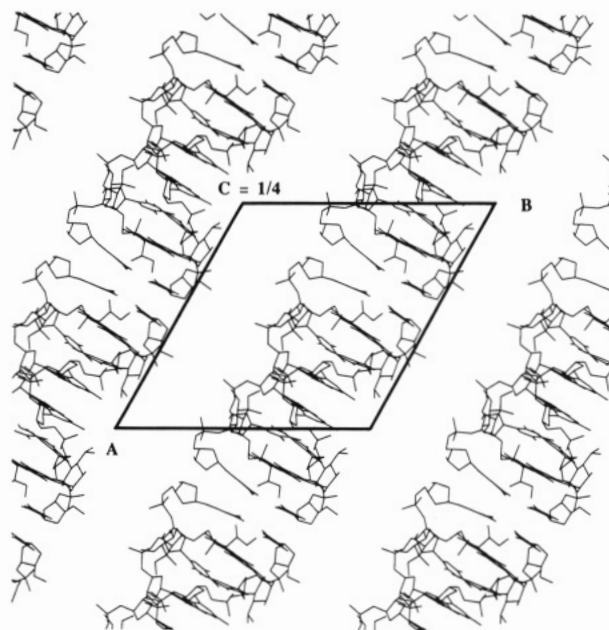

FIGURE 9: Packing arrangement in the crystal lattice of the DNA–nogalamycin complex. This drawing shows an *xy* layer of approximately 20-Å thickness centered on $z = {}^1/_4$. The unit cell is outlined by a heavy line.

C(1) and to a phosphate oxygen of G(2). Water molecule 28 donates protons in hydrogen bonds to O3′ of G(12) and to O1′ of the nogalose. Water molecule 35 donates protons in hydrogen bonds to O4′ of the nogalose and to O3′ of T(3). Water molecule 37 accepts protons in hydrogen bonds to the positively charged N1 of the bicyclo amino sugar and to the N6 of A(10). The water molecules engaged in multidentate hydrogen bonds, with the exception of water 35, have relatively low temperature factors (Table V). This exception can be explained by the formation of an unfavorable contact between water 35 and O2P of A(10). The contact is not a hydrogen bond as the phosphate can only accept protons in hydrogen bonds and water molecule 35 donates in two other hydrogen bonds as described above.

Crystal Packing. The DNA–nogalamycin complexes form infinite stacks which lie parallel to the *a* axis with two duplexes stacking in a 3′,3′ and 5′,5′ manner (Figure 9). All the

complexes within a layer are related by translations, and all the complexes within a stack are related by translations or rotations. The crystallographic 2-fold rotation axes in this layer are normal to the *a* axis and pass alternately between and through the complexes. In Figure 9, the major groove of each complex opens to the right. Adjacent stacks are separated by roughly 3 Å. Close intermolecular contacts occur primarily between the ends of duplexes with slightly smaller distances between adjacent guanines than between cytosines. Between stacked guanines, there are two close contacts. The distance from N1 [G(12)] to C6 [C(6*)] is 3.12 Å and to O6 [G(6*)] is 2.93 Å. The distances between adjacent cytosines are all longer than 3.4Å.

The packing diagram (Figure 9) shows that there are no close contacts between stacks of the same layer. However, between layers (not shown) a close contact of 2.88 Å occurs between O1P [G(2)] and C10′ of a symmetry-related complex (symmetry operator: $[x - y, x, z + 1/6]$). Thus, the complexes are fully hydrated and nearly totally surrounded by water. It is interesting to note that the nogalamycin complex is different from the complex of 11-deoxydaunomycin with d(CGTsACG) (Williams et al., 1990b), where the thioated phosphate group is engaged in a water-mediated lattice contact. As the methylation at both cytosines does not lead to any specific changes regarding the packing, these modifications do not seem to be of great importance with respect to different crystallization behavior.

DISCUSSION

To accommodate intercalation of the nogalamycin chromophore, the DNA helix elongates, translocating the base pairs in the approximate direction of the helical axis. However, the hydrogen bonds of the base pairs form flexible hinges permitting differential movement of the centers and the edges of the base pairs. The centers of the base pairs move further along the helical axis than do the edges. The result is a marked lack of planarity of the base pairs surrounding the intercalation site.

The interaction of nogalamycin with DNA is novel because the functional groups of this drug are not present in other intercalating drugs cocrystallized with DNA fragments to date. The three-dimensional shape of nogalamycin provides a surprisingly poor fit in the complex with DNA. The long axis of nogalamycin exceeds the width of the DNA helix. To accommodate this poor fit, both the DNA and nogalamycin assume strained conformations in the ground state complex. Even so, the potential for stabilizing interactions is not achieved and the nogalose sugar "floats" in the minor groove, almost without contacting the DNA. This poor fit could serve several biological functions. In a complex with a long fragment of DNA, helical distortion by nogalamycin could be transmitted for long distances down the helix, effecting interactions with other biological macromolecules. In addition, the poor fit of nogalamycin with DNA serves to destabilize the complex and ensures that the DNA–drug complex forms reversibly. The large surface area gives nogalamycin the potential to form extremely stable and potentially irreversible complexes with DNA. The poor fit ensures reversible binding to DNA, a common and apparently effective mode of binding of biological antimicrobial agents.

With the assumption that transient DNA melting is required for entry of nogalamycin, it has been proposed that sequence specificity of nogalamycin binding may be determined by the effects of sequence on duplex stability (Liaw et al., 1989). In this model, nogalamycin binds with greater affinity to low-melting DNA (AT rich) than to high-melting DNA (GC rich).

However, this analysis incorporates a requirement for DNA melting during entry of nogalamycin but neglects the commensurate requirement for DNA melting during exit of nogalamycin. If transient melting of the duplex is required for entry of nogalamycin into DNA, it also must be required for exit and, therefore, duplex stability should affect the kinetics of association and dissociation but not necessarily the thermodynamics of the ground-state complex. Thus, the proposed relationship between duplex stability and nogalamycin specificity is improbable.

The hydrogen-bonding interactions between nogalamycin and DNA do not suggest that the binding is sequence specific. Two hydroxyl groups of nogalamycin form hydrogen bonds into the major groove. As hydroxyl groups can both donate or accept hydrogen bonds, these hydrogen bonds to the major groove would be nonspecific.

The greatest conformational changes induced by binding to DNA are observed in the regions of the nogalamycin molecule that interact most strongly with the DNA and thus appear to be direct consequences of the interactions with DNA. The greatest changes in nogalamycin involve the bicyclo amino sugar and the methyl ester, the two domains that form direct hydrogen bonds to the DNA. The adjustments of the methyl ester and bicyclo amino sugar both serve to swing these functional groups toward the center of the nogalamycin molecule. Thus, nogalamycin "clamps" onto the DNA helix. The total distance of the clamping action is 1.4 Å, which is the difference in the distances from O4″ to O14 in bound versus unbound nogalamycin. It is unlikely that this clamping action occurs without an energetic cost as the torsional changes involve fused ring systems. However, the clamping action is apparently required by the discrepancy in the length of nogalamycin and the width of the DNA duplex.

More moderate conformational changes are induced in those regions of the nogalamycin molecule which interact weakly with the DNA. The torsional changes at the glycosyl linkage are modest (Table I) although the position of the nogalose sugar should be relatively unrestrained as the energetic barrier to rotation about the glycosyl linkage of the A ring to the nogalose is low.

In general, base pair buckling is the most severe alteration along the helical axis resulting from intercalation [also see Quigley et al. (1980)]. The buckle of 26° of the G(2)·C(11) base pair is particularly striking (Figure 7B,C, right). The most severe buckle in daunomycin-type complexes is considerably less [16° (Frederick et al., 1990)]. Whereas buckle is observed in all DNA–intercalator complexes, the propeller twist is variable and is slightly larger in the daunomycin-type complexes (Frederick et al., 1990) than in the nogalamycin complex (Figure 7, right). In the nogalamycin complex the base pairs are more highly sheared (Figure 7B,C, left) than those in daunomycin-type complexes, which exhibit almost no shear (Frederick et al., 1990).

Intercalation Unwinds DNA. Contradictory to the description but in accordance to the numerical data of the previous report (Williams et al., 1990a), nogalamycin unwinds DNA at the step adjacent to the intercalation site [i.e., the G(2)·C(11)–T(3)·A(10) step] but not at the intercalation step.[2] Thus nogalamycin and daunomycin unwind DNA in similar fashions. However, compared to daunomycin-type complexes, in the nogalamycin complex there is considerably more unwinding at this step. Viewing down the helical axis, unwinding of the DNA causes the ribose of one residue to be shifted

toward the ribose of the next residue. Displacement of a base pair in its plane can lead to asymmetric shifts of this type, affecting one strand more than the other. In intercalated DNA complexes, the backbones are shifted at specific sites around the intercalator. The shifts are generally not symmetric. A hydrogen bond between either nogalamycin or daunomycin and the N2 of a guanine appears to displace the base pair toward the minor groove, leading to asymmetric shifts of the backbone. The variations in DNA torsion angles around the intercalation sites give a measure of the asymmetry of the two backbones. Certain torsion angles vary considerably from residue to residue, demonstrating the flexible nature of the backbone.

Less shearing of base pairs is observed in a related nogalamycin complex without 5-methyl groups on the cytosines and in a different crystal form (Liaw et al., 1989). That structure shows more similarity with the daunomycin complex. The authors report a weak hydrogen bond between the ester group and G(12) in the minor groove and only one hydrogen bond between the amino sugar and the G(2)·C(11) pair, with the distance between O4″ and N4 of C11 given as 3.58 Å. The origin of the differences between the complexes is not quite clear. Nogalamycin may have two distinct positions in the DNA complex, or alternatively, it is possible that hydrogen bond constraints used in the refinement may influence the final conformation.

Binding of nogalamycin causes both the major and the minor groove to widen compared to the standard duplex (Table IV). Although the backbone angles are significantly altered as a result of the penetration of an intercalator, the distances between adjacent phosphorus atoms are nearly constant and are not much different from those in standard B-DNA. This holds for all DNA-intercalator complexes crystallized thus far. It appears that even severe distortions of the backbone do not necessarily change the relative positions of the phosphorus atoms, suggesting that their arrangement is mainly governed by electrostatic interactions.

Water-mediated hydrogen bonds are those in which a water molecule simultaneously forms at least two hydrogen bonds to the drug and/or to the DNA. As the number of ligands bound to a water molecule approaches four, both the location of the water molecule and its hydrogen bond donor/acceptor interactions can be fully determined by the ligands. There are four examples of multidentate hydrogen bonding to water molecules in the nogalamycin-DNA complex. With one exception, the temperature factors of each of these water molecules are low, as expected for tightly bound solvent molecules. In the exception, an unfavorable contact with a phosphate oxygen destabilizes the bound water molecule.

The patterns of thermal motion suggest that the conformations of DNA-drug complexes represent those of isolated complexes in solution which are not distorted by lattice effects. The terminal regions of the complexes, where the lattice forces are greatest, have larger thermal motions than the central regions. The patterns of thermal motion of the backbone but not of the bases are similar in the nogalamycin complex to those in daunomycin-type complexes which crystallize in a different crystal form. In the crystal structures of complexes of daunomycin and adriamycin with the DNA hexamer d-(CGATCG) (Frederick et al., 1990), the differences in thermal motion between residues are smaller, but, in both cases, backbone atoms at the end of the duplex show larger amplitudes. The complex between 11-deoxydaunomycin and the DNA hexamer d(CGTsACG) in a third crystal form (Williams et al., 1990b) shows a pattern of thermal motion nearly identical with that of the nogalamycin complex, with the motion at the ends of the duplex being much larger than the motion in the center of the duplex.

REFERENCES

Acramone, F., & Penco, S. (1988) in *Anthracycline and Anthracenedione Based Anticancer Agents* (Lown, J. W., Ed.) pp 1–43, Elsevier, New York.

Arora, S. K. (1983) *J. Am. Chem. Soc. 105*, 1328–1332.

Bhuyan, B. K. (1967) in *Antibiotics* (Gottlieb, D., & Shaw, P. D., Eds.) Vol. 1, pp 173–180, Springer, New York.

Bhuyan, B. K., & Reusser, F. (1970) *Cancer Res. 30*, 984–989.

Brooks, B. R., Bruccoleri, R. E., Olafson, B. D., States, D. J., Swaminathan, S., & Karplus, M. (1983) *J. Comput. Chem. 4*, 187–217.

Brown, J. R. (1983) in *Molecular Aspects of Anti-Cancer Drug Action* (Neidle S., & Waring M. J., Eds.) pp 57–92, Macmillan Press, London.

Brünger, A. T., Kuriyan, J., & Karplus, M. (1987) *Science 235*, 458–460.

Collier, D. A., Neidle, S., & Brown, J. R. (1984) *Biochem. Pharmacol. 33*, 2877–2880.

Conner, B. N., Takano, T., Tanaka, S., Itakura, K., & Dickerson, R. E. (1982) *Nature (London) 295*, 294–299.

Das, G. C., Dasgupta, S., & Das Gupta, N. N. (1974) *Biochim. Biophys. Acta 353*, 274–282.

Dickerson, R. E., et al. (1989) *Nucleic Acids Res. 17*, 1797–1803.

Ennis, H. L. (1981) *Antimicrob. Agents Chemother. 19*, 657–665.

Fok, J., & Waring, M. J. (1972) *Mol. Pharmacol. 8*, 65–74.

Fox, K. R., Brasset, C., & Waring, M. J. (1985) *Biochim. Biophys. Acta 840*, 383–392.

Frederick, C. A., Williams, L. D., Ughetto, G., van der Marel, G. A., van Boom, J. H., Rich, A., & Wang, A. H.-J. (1990) *Biochemistry 29*, 2538–2549.

Gale, E. F., Cundliffe, E., Reynolds, P. E., Richmond, M. H., & Waring, M. J. (1981) in *The Molecular Basis of Antibiotic Action* (Neidle, S., & Waring, M. J., Eds.) pp 285–401, Wiley, London.

Hendrickson, W. A., & Konnert, J. H. (1981) in *Biomolecular Structure, Conformation, Function and Evolution* (Srinivasan, R., Ed.) pp 43–57, Pergamon, Oxford.

Jones, T. A. (1978) *J. Appl. Crystallogr. 11*, 268–272.

Kersten, W., Kersten, H., & Szybalski, W. (1966) *Biochemistry 5*, 236–244.

Li, L. H., Kuentzel, S. L., Murch, L. L., Pschigoda, L. M., & Krueger, W. C. (1979) *Cancer Res. 39*, 4816–4822.

Liaw, Y.-C., Gao, Y.-G., Robinson, H., van der Marel, G. A., van Boom, J. H., & Wang, A. H.-J. (1989) *Biochemistry 28*, 9913–9918.

Plumbridge, T. W., & Brown, J. R. (1979) *Biochem. Pharmacol. 28*, 3231–3234.

Quigley, G. J., Teeter, M. M., & Rich, A. (1978) *Proc. Natl. Acad. Sci. U.S.A. 75*, 64–68.

Quigley, G. J., Wang, A. H.-J., Ughetto, G., van der Marel, G. A., van Boom, J. H., & Rich, A. (1980) *Proc. Natl. Acad. Sci. U.S.A. 77*, 7204–7208.

Saenger, W. (1984) *Principles of Nucleic Acid Structure*, p
266, Springer-Verlag, New York.
Searle, M. S., Hall, J. G., Denny, W. A., & Wakelin, L. P.
G. (1988) *Biochemistry 27*, 4340–4349.
Sinha, R. K., Talapatra, P., Mitra, A., & Mazumder, S.
(1977) *Biochim. Biophys. Acta 474*, 199–209.
Wang, A. H.-J., Ughetto, G., Quigley, G. J., & Rich, A.
(1987) *Biochemistry 26*, 1152–1163.

Waring, M. J. (1970) *J. Mol. Biol. 54*, 247–279.
Williams, L. D., Egli, M., Gao, Q., Bash, P., van der Marel,
G. A., van Boom, J. H., Rich, A., & Frederick, C. A.
(1990a) *Proc. Natl. Acad. Sci. U.S.A. 87*, 2225–2229.
Williams, L. D., Egli, M., Ughetto, G., van der Marel, G. A.,
van Boom, J. H., Quigley, G. J., Wang, A. H.-J., Rich, A.,
& Frederick, C. A. (1990b) *J. Mol. Biol. 215*, 313–320.
Zhang, X., & Patel, D. J. (1990) *Biochemistry 29*, 9451–9466.

Interaction of Berenil with the *Eco*RI Dodecamer d(CGCGAATTCGCG)2 in Solution Studied by NMR[†]

Andrew N. Lane,[*,‡] Terence C. Jenkins,[*,§] Tom Brown,[‖] and Stephen Neidle[§]

Laboratory of Molecular Structure, National Institute for Medical Research, The Ridgeway, Mill Hill, London NW7 1AA,
U.K., Cancer Research Campaign Biomolecular Structure Unit, Institute of Cancer Research, Sutton, Surrey SM2 5NG, U.K.,
and Department of Chemistry, University of Edinburgh, Edinburgh EH9 3JJ, U.K.

Received July 10, 1990; Revised Manuscript Received September 11, 1990

ABSTRACT: The conformation of the *Eco*RI dodecamer d(CGCGAATTCGCG)2 has been examined in
solution by ^{1}H and ^{31}P NMR. Spin–spin coupling constants and nuclear Overhauser (NOE) enhancement
spectroscopy show that all deoxyriboses lie in the south domain, with a small admixture of the north
conformation (0–20%). The time dependence of the nuclear Overhauser enhancements also reveals a relatively
uniform conformation at the glycosidic bonds (average angle, $\chi = -114°$). The average helical twist is 36.5°
(9.8 base pairs per turn). Tilt angles are small (in the range 0 to −10°), and roll angles are poorly determined.
Unlike single-crystal X-ray studies of the same sequence, there is no evidence for asymmetry in the structure.
Both the NOE intensities and ^{31}P relaxation data imply conformational anomalies at the C3–G4/C9–G10
and the A5–A6/T7–T8 steps. Berenil binds in 1:1 stoichiometry to the dodecamer with high affinity (K_d
= 1 μM at 298 K) and causes substantial changes in chemical shifts of the sugar protons of nucleotides
Ado 5–Cyt 9 and of the H2 resonances of the two Ado residues. No significant asymmetry appears to be
induced in the DNA conformation on binding, and there is no evidence for intercalation, although the binding
site is not centrosymmetric. NOEs are observed between the aromatic protons of berenil and the H1′ of
both Thy 7 and Thy 8, as well as to Ado 5 and Ado 6 H2. These results firmly establish that berenil binds
via the minor groove and closely approaches the nucleotides Ado 6, Thy 7, and Thy 8. On the basis of
quantitative NOE spectroscopy and measurements of spin–spin coupling constants, changes in the con-
formations of the nucleotides are found to be small. Using the observed NOEs between the ligand and the
DNA together with the derived glycosidic torsion angles, we have built models that satisfy all of the available
solution data. The berenil molecule binds at the 5′-AAT (≡5′-ATT on the complementary strand) site
such that (i) favorable hydrogen bonds are formed between the charged amidinium groups and the N3 atoms
of Ado 6 and Ado 18 and (ii) the ligand is closely isohelical with the floor of the minor groove.

N MR has been shown to be an excellent method for stud-
ying the interactions of ligands such as drugs with DNA
fragments (Gao & Patel, 1989). Numerous investigations have
determined the mode of interaction of intercalators and groove
binding agents with DNA and the conformational conse-
quences of binding.

Berenil [1,3-bis(4′-amidinophenyl)triazene, diminazene,
structure I] is a DNA minor groove binding compound with

I
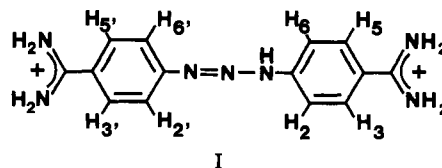
mild cytotoxic and antiviral properties (De Clercq & Dann,
1980) that is used extensively for the treatment of bovine
trypanosomiasis. The compound shows preferential affinity
for AT-rich tracts of DNA (Zimmer & Wähnert, 1986), and
binding to double-stranded DNA has long been implicated in
these biological effects. The interaction of berenil with DNA
has been confirmed by DNase I and hydroxyl radical foot-
printing studies with a *Tyr* T fragment (Portugal & Waring,
1987; Laughton et al., 1990), which have revealed that the

*To whom correspondence (either author) should be addressed.
[‡]National Institute for Medical Research.
[§]Institute of Cancer Research.
[‖]University of Edinburgh.